ORGANOMETALLICS

pubs.acs.org/Organometallics Article

Synthesis and Structure of Arene Ru(II) N^O-Chelating Complexes: *In Vitro* Cytotoxicity and Cancer Cell Death Mechanism

Sundarraman Balaji, Mohamed Kasim Mohamed Subarkhan, Rengan Ramesh,* Hangxiang Wang, and David Semeril

Cite This: https://dx.doi.org/10.1021/acs.organomet.0c00092 Read Online

ACCESS | Metrics & More | Article Recommendations | Supporting Information

ABSTRACT: A panel of six new structurally related organometallic arene Ru(II) complexes of general composition [(η^6-benzene)Ru(L)Cl] (**1**–**3**) and [(η^6-*p*-cymene)Ru(L)Cl] (**4**–**6**) (L = dimethylaminobenzhydrazones) have been designed and synthesized in search of new ruthenium anticancer drugs. The identities of the synthesized complexes have been well-established by elemental analysis and various spectral (FT-IR, UV–vis, NMR, and HR-MS) methods. The solid-state molecular structures of the ruthenium complexes were determined with the help of X-ray crystallography and confirms the presence of a pseudo-octahedral geometry around ruthenium. Furthermore, cytotoxicity of the complexes has been unveiled with the aid of MTT assay against A549 (lung carcinoma), LoVo (colon adenocarcinoma), HuH-7 (hepato cellular carcinoma) along with the noncancerous 16HBE (human lung bronchial epithelium) cells and compared with the effect of the standard drug cisplatin. Interestingly, complexes **4**, **5**, and **6** which contain a *p*-cymene moiety induce a remarkable decrease of cell viability against all the cancer cells tested. The capacity corresponding to the inhibition of A549 cells proliferation was analyzed by 5-ethynyl-2-deoxyuridine (EdU) incorporation assay and indicated a notable effect of *p*-cymene counterparts **4**, **5**, and **6** over cisplatin. Further studies such as AO-EB (acridine orange–ethidium bromide) staining, flow cytometry, and Western blot analyses on cell death mechanism signified that the cytotoxicity was associated with apoptosis in cancer cells. This clearly suggests that *p*-cymene-capped Ru(II) complexes are also one of the propitious cancer therapeutic candidates and are worthy of further investigations.

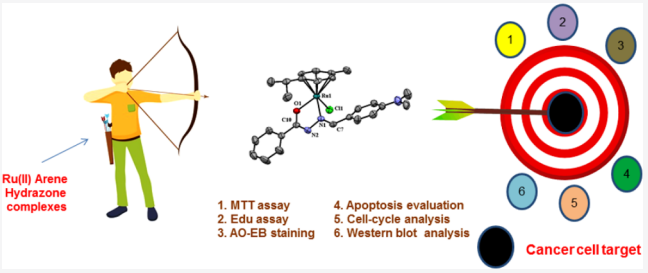

INTRODUCTION

GLOBOCAN estimates 36 types of cancers in 185 countries based on the incidence, mortality and prevalence in the year 2019. Nowadays, chemotherapy is the most widely used cancer treatment among radio, immune, hormone, and gene therapies.[1] Though many platinum-based anticancer drugs are known, most of them are associated with adverse effects.[2] Owing to this unsatisfactory treatment of platinum-based drugs in the scenario of undesirable side effects, scientists search non-platinum-metal-based drugs with target specificity, less toxicity toward healthy cells, and potent activity against a wide assortment of cancers.[3] In the exploration of novel anticancer drugs, great interest has been raised on ruthenium complexes, and these are being tested on several cancer cells.[4−6]

Ruthenium complexes are considered one of the best alternatives to their platinum counterparts by following rationales such as effectivity toward some cisplatin-resistant cancers,[7] and high selectivity toward cancer cells/targets, as well as having minimal side effects and being mimetic of iron in binding targets.[8] Ruthenium-based drug KP1019 entered phase I clinical trial, and its further development is limited due to low solubility.[9] Yet another drug, NAMI-A, succeeded in phase I clinical studies and showed only limited efficacy in phase II clinical trial.[10] Moreover, other ruthenium drugs KP1339,[11] TLD-1433,[12] RM175,[13] RAPTA-C,[14] and RAED[15] are under (pre)clinical studies (Figure 1). Low-spin d^6 arene ruthenium complexes have attracted great interest in cancer metallotherapeutics due to the structural diversity in ancillary ligands and easy accessibility on the hydrophobic nature of arene by substitutions.[16] Recently, many ruthenium complexes appended arene moiety were reported as potent anticancer agents.[17] Intense investigations were focused on ligands such as arene, phosphine, and other multidentate ligands containing oxygen, nitrogen, and sulfur.[18−21]

Schiff bases can coordinate to metal centers and exhibit different coordination modes which lead to the production of many mono- and binuclear complexes with diverse stereochemical properties.[22] Metal hydrazone complexes can have a wide range of structures with different coordination numbers,

Received: February 11, 2020

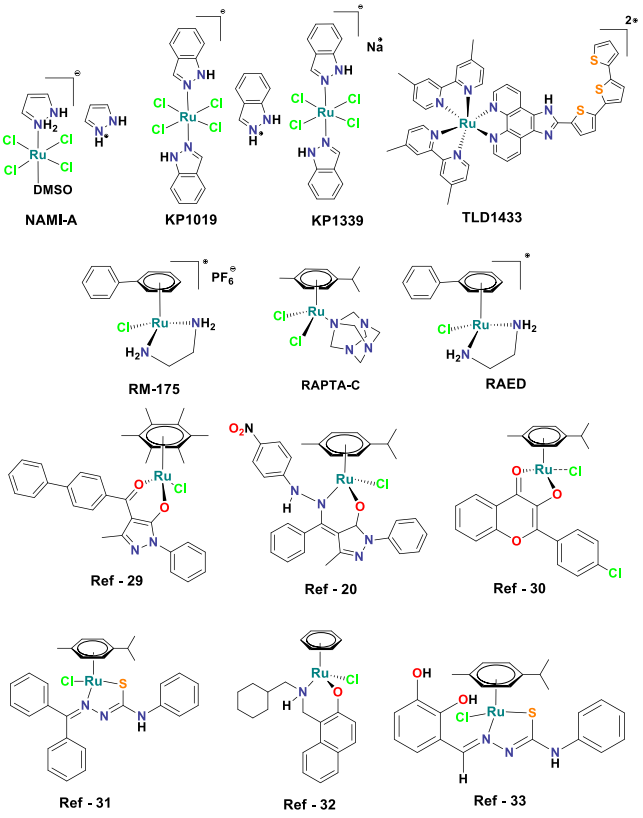

Figure 1. Examples of some ruthenium-based anticancer complexes.[20,29−33]

geometries, and accessible redox states.[23] Furthermore, ruthenium hydrazone complexes exhibit a broad spectrum of significant biological activities as anticancer, antitumor, antifungal, antibacterial, antimicrobial, antioxidant, herbicidal, insecticidal, and plant stimulant properties, as well as being present in natural oxygen carriers.[19,24−26] In addition, the compounds possessing a *p*-dimethylaminophenyl moiety exhibit antinociceptive and analgesic activities.[27,28]

Pettinari et al. found that the Ru(II)−arene-acylpyrazolonato complex exhibits efficient cytotoxicityonvarious cancer cell lines (HeLa, MCF-7, HepG2, and HCT-116; IC_{50} = 13−30 μM).[29] Recently, the same authors have reported antiproliferative activity of half-sandwich Ru(II) complexes with *N,O*- or *N,N*-pyrazolone-based hydrazones ligands against MCF-10A, MCF-7, HeLa, and HCT116 cancer cell lines (IC_{50} = 10−175 μM).[20] The synthesis and antiproliferative activity of $Ru^{II}(\eta^6$-arene) compounds carrying bioactive flavonol ligands have been reported by Hartinger et al. (CH1, SW480, A549, 5637, LCLC-103H, and DAN-G; IC_{50} = 0.86−19 μM).[30] Wei Su et al. have described the DNA binding properties and anticancer activity of arene ruthenium(II) complexes bearing ketone-*N*4-substituted thiosemicarbazones (SGC-7901, BEL-7404, and HEK-293T; IC_{50} = 10−17 μM).[31] Furthermore, Castonguay and his co-workers have reported the synthesis of novel ruthenium half-sandwich complexes containing (*N,O*)-bound Schiff base ligands with moderate anticancer activity (A2780, SH-SY5Y, MCF-7, T47D, and MCF-12A; IC_{50} = 8.9−59.3 μM).[32] Sadler and his co-workers have reported the solution behavior and antiproliferative activity of arene ruthenium thiosemicarbazone complexes against A2780, A2780 Cis, A549, HCT116, and PC3 cancer cell lines (IC_{50} = 0.36−1.64 μM).[33] Recently, our research group has explored the synthesis, antiproliferative activity, and cancer cell death mechanism of arene Ru(II) complexes featuring benzhydrazones.[34] In the present work, we report the synthesis and structural chracterisation of arene Ru(II) complexes containing 4-dimethylamino benzhydrazones. Furthermore, the cytotoxicity of the complexes toward the A549, LoVo, HuH-7 and noncancerous 16HBE cells has been examined and the cancer cell death mechanism was investigated by various biochemical assays.

RESULTS AND DISCUSSION

Three hydrazone ligand derivatives have been easily obtained in good yields from the reaction of 4-(dimethylamino)-benzaldehyde with substituted benzhydrazides in an equimolar ratio. Metalation was accomplished by reacting the ruthenium(II) arene precursors $[(\eta^6$-arene)$RuCl(\mu$-$Cl)]_2$ (arene = benzene or *p*-cymene) and hydrazones in a 0.5:1 molar ratio respectively with 1 equiv of Et_3N base (Scheme 1).

Scheme 1. Synthesis of Arene Ru(II) Complexes

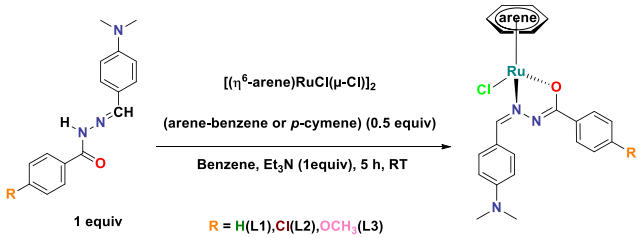

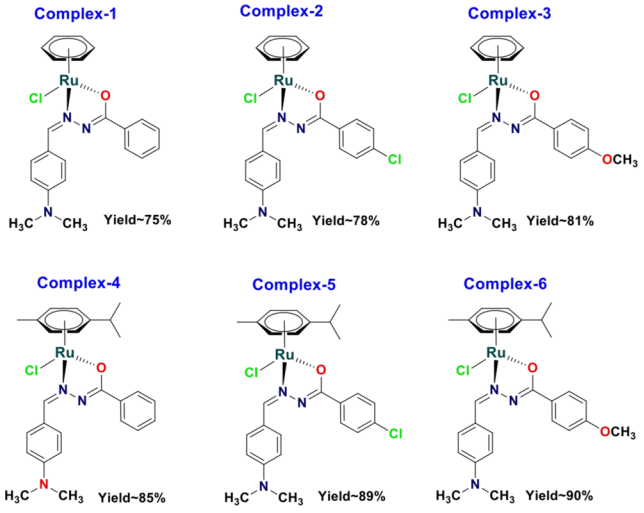

Figure 2. Chemical structures of arene Ru(II) benzhydrazone complexes **1**−**6**.

Ruthenium hydrazone complexes **1**−**6** (Figure 2) of the general formula $[(\eta^6$-arene)Ru(L)Cl], where L= substituted dimethylaminobenzhydrazone derivatives, were collected in good yields. The presence of Et_3N in the reaction mixture facilitates the amido-imidol tautomerization for easy coordination of imidolate oxygen. All complexes were found to be stable in air and were readily dissolved in most organic solvents including acetonitrile, EtOH, MeOH, $CHCl_3$, DMF, DMSO, and so on. The formation new ruthenium complexes was

https://dx.doi.org/10.1021/acs.organomet.0c00092
Organometallics XXXX, XXX, XXX−XXX

authenticated with the aid of analytical and various spectral techniques.

The ν_{N-H}'s of the free ligands show bands in the region of 3242−3427 cm^{-1}. Furthermore, the ligands displayed $\nu_{CH=N}$ and $\nu_{C=O}$ IR absorptions in the regions of 1546−1601 cm^{-1} and 1653−1661 cm^{-1}, respectively, indicated that the ligand exists in its amide form (Figures S1−S9). Upon complexation, the ν_{N-H} and $\nu_{C=O}$ bands disappeared, which indicated that the ligand underwent amido-imidol tautomerization and subsequent coordination in its imidol form. This was further supported by appearance of a C−O band around 1340−1370 cm^{-1}. Coordination of the azomethine nitrogen to the ruthenium metal center was corroborated by a decrease of $\nu_{CH=N}$ absorption frequency in the region of 1500−1530 cm^{-1}.

Furthermore, ^{1}H NMR spectra of the complexes support the binding nature of the ligand to metal ion (Figures S19−S24). Multiplets observed in the region of 6.68−8.10 ppm were due to the aromatic protons of benzhydrazone ligands. The appearance of a sharp singlet in the region of 8.80−8.88 ppm has been assigned to the azomethine proton. This signal slightly shifted from a lower to a higher frequency during complexation, which revealed that azomethine nitrogen is one of the coordinating atoms to ruthenium center. The disappearance of signal due to −NH protons of the free ligands in the region of 10.29−11.55 ppm indicated amido-imidol tautomerism and subsequent coordination of the imidolate oxygen atom. Hence, spectral data clearly indicated that the ligands bind to the ruthenium ion through the coordination of nitrogen of azomethine group and the imidolate oxygen. Furthermore, the aromatic protons of benzene moiety in complexes **1**−**3** displayed a singlet in region of 5.37−5.44 ppm. The *p*-cymene ring protons were observed as doublets at 4.68−5.43 ppm for complexes **4**−**6**. In addition, a doublet of doublet in the region of 1.11−1.15 ppm was appeared due to isopropyl methyl protons of the *p*-cymene, and the −CH of isopropyl group was displayed as a septet in the region of 2.29−2.67 ppm. Complexes **3** and **6** exhibited methoxy signals of the benzhydrazone ring as singlets around 3.80 ppm. ^{13}C{H} NMR of the complexes showed resonances in the expected region (Figures S25−S30). A higher frequency shift (160.3−161.4 ppm) obtained for all the complexes due to imine carbon (−C═N−) in comparison with free ligands (148.0−149.8 ppm) indicated the coordination of the imine nitrogen to the ruthenium ion. Furthermore, shifting of the signal from a lower frequency of 161.6−164.3 ppm to a higher frequency of 171.9−173.3 ppm due to the reduction of the bond order (−N═C−O) upon complexation when compared to free ligands (−NH−C═O).

The absorption spectra of the complexes were monitored in acetonitrile in the range of 800−200 nm at room temperature and showed three bands with absorption maxima in the region of 230−389 nm. Two ligand based transitions such as $\pi-\pi^*$ and $n-\pi^*$ were observed around 230−294 nm. Bands with medium intensity which appeared in the region of 383−389 nm are ascribed to MLCT transitions (Figures S31−S36). The outline of the absorption spectra of all the complexes looks similar to those of other reported octahedral arene ruthenium(II) complexes.[26c,20]

Furthermore, HR-MS analysis was performed under positive ion ESI-MS mode in acetonitrile. The mass spectral data confirmed the composition of synthesized complexes **1**−**6** (Figures S37−S44) displayed peaks at *m*/*z* 446.08 $[M - Cl]^+$, 516.01 $[M + H]^+$, 476.09 $[M - Cl]^+$, 538.11 $[M + H]^+$, 572.08 $[M + H]^+$, and 568.12 $[M + H]^+$, respectively, confirmingthe presence of the expected moiety in the solution phase. Hence, the mass spectral data are in good concord with the molecular formula proposed for all the complexes.

X-ray Crystallographic Studies. Two of the complexes, **1** and **4**, were isolated as single crystals by the slow evaporation of the 1:2 CH_2Cl_2/petroleum ether mixture at room temperature, and their molecular structures were studied with the aid of crystallographic technique. Crystal data and refinement parameters were given in Table S1. The selected bond lengths and bond angles were gathered in Table S2. From the unit cell parameters, it was obvious that the crystal system of complex **1** was orthorhombic, belonging to the *Pbca* space group, and **4** was monoclinic with the $P2_1/c$ space group. The ORTEP views of the complexes **1** and **4** were shown as thermal ellipsoids in Figures 3 and 4 respectively, which clearly

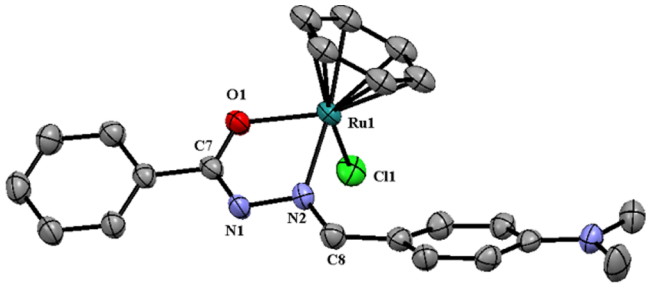

Figure 3. ORTEP view of the complex **1** with 30% probability. All the hydrogen atoms were omitted for clarity. Bond angles around Ru(II) ion: O(1)−Ru(1)−N(2) = 76.74(9)°, O(1)−Ru(1)−Cl(1) = 85.99(6)°, N(2)−Ru(1)−Cl(1) = 88.79(7)°. Bond lengths: N(2)−Ru(1) = 2.112(3)Å, O(1)−Ru(1) = 2.060(2)Å, Cl(1)−Ru(1) = 2.4116(9)Å.

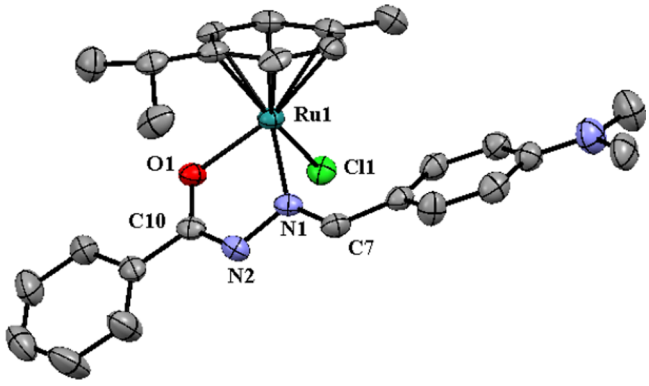

Figure 4. ORTEP view of the complex **4** with 30% probability. All the hydrogen atoms were omitted for clarity. Bond angles around Ru(I) ion: O(1)−Ru(1)−N(1) = 76.73(12)°, O(1)−Ru(1)−Cl(1) = 84.89(8)°, N(1)−Ru(1)−Cl(1) = 85.88(10)°. Bond lengths: N(1)−Ru(1) = 2.096(3)Å, O(1)−Ru(1) = 2.054(2)Å, Cl(1)−Ru(1) = 2.4028(11)Å.

indicated that ruthenium was coordinated by the ligand via the imine nitrogen and imidolate oxygen with the formation of a five-member chelate ring with bite angles of 76.73(12)−76.74(9)° in a piano-stool geometry. While the seat of the piano stool was made by the arene ring, the N^O bidentate benzhydrazone and Cl ligands fashioned the three legs of the stool. Ru−centroid distances fall in the range 1.656−1.677 Å, and this is in agreement with already reported Ru(II) arene

https://dx.doi.org/10.1021/acs.organomet.0c00092
Organometallics XXXX, XXX, XXX−XXX

Table 1. *In Vitro* Cytotoxic Effect of Arene Ru(II) Benzhydrazone Complexes after 72 h of Incubation (IC_{50} ± SD, μM) and Their Calculated Partition Coefficients (log *P*)[a]

	A549 (SI)	LoVo (SI)	HuH-7 (SI)	16HBE	log *P*
complex **1**	12.63 ± 0.49 (2.17)	25.04 ± 1.83 (1.09)	19.74 ± 1.12 (1.39)	27.52 ± 1.16	1.68 ± 0.06
complex **2**	13.85 ± 0.77 (2.04)	21.91 ± 1.55 (1.29)	22.14 ± 1.37 (1.28)	28. 37 ± 2.16	1.94 ± 0.07
complex **3**	9.92 ± 0.98 (2.20)	17.88 ± 1.03 (1.22)	12.78 ± 0.51 (1.71)	21.88 ± 1.39	1.48 ± 0.01
complex **4**	7.15 ± 0.78 (5.02)	8.21 ± 0.86 (4.38)	7.43 ± 0.48 (4.83)	35.96 ± 0.57	1.28 ± 0.03
complex **5**	7.73 ± 0.58 (3.23)	6.92 ± 0.61 (3.61)	8.74 ± 0.68 (2.86)	25.04 ± 0.81	1.31 ± 0.05
complex **6**	6.52 ± 0.69 (3.36)	5.62 ± 0.49 (3.89)	5.37 ± 0.56 (4.08)	21.91 ± 0.71	1.19 ± 0.02
cisplatin	8.72 ± 0.74 (2.05)	10.95 ± 0.67 (1.63)	10.68 ± 0.68 (1.67)	17.88 ± 1.12	−1.95 ± 0.09

[a]Selectivity index (SI) is defined as IC_{50} ratio of non-cancerous cells (16HBE) to cancerous cells (A549, LoVo and HuH-7).

complexes.[20,35] The σ-bond lengths of three legs of the stool, Ru−N, Ru−O, and Ru−Cl, and the corresponding bond angles correspond with other structurally related benzene and *p*-cymene ruthenium complexes encompassing similar piano-stool geometry.[36]

Stability Study. It is essential to study the stability of metal complexes in aqueous media for drug development in clinical investigations. The stability of ruthenium complexes in aqueous solution was determined using UV−visible spectrophotometry at various time intervals. The complexes were taken in a solution of 1% dimethyl sulfoxide in phosphate buffer at pH 7.4, and the representative spectra were given in Figure S43. It has been observed from the spectral diagram that there was no significant change over 72 h intervals, evidencing the stability of the complexes and their fate under physiological conditions; hence, they were subjected to further studies.

Partition Coefficient Determination (Lipophilicity). The lipophilicity is an important factor to determine the cell membrane permeation capacity of the complexes and is studied in terms of the partition coefficient (log *P*). It is based on the solubility and distribution of the complexes in an *n*-octanol/water system. From the calculated log *P* values of complexes **1**−**6** (Table 1), it was observed that the complexes are likely to differ in their lipophilicity which might be due to the variation in the different arene moieties and the nature of the substituent in the ligands. Furthermore, complexes **4**−**6** which comprise *p*-cymene moiety showed higher lipophilicity than the rest of the benzene complexes suggested that the substituents on arene ring enhanced the lipophilicity. The observed log *P* values for the complexes and cisplatin are in agreement with the reported ruthenium complexes.[37]

***In Vitro* Cytotoxicity by MTT Assay.** To check the potency of the complexes in retarding the growth of cancer cells, MTT assay was carried out with A549 (lung carcinoma), LoVo (colon adenocarcinoma), HuH-7 (hepato cellular carcinoma), and noncancerous 16HBE (human lung bronchial epithelium) cells over 72 h (Figure S44). No inhibition of the cell growth was observed by the free ligands or ruthenium precursor even up to 100 μM. Hence, chelation plays an important role in the observed cytotoxicity of the complexes. Most of the complexes exhibit potent cytotoxicity against the tested cancer cells (Table 1). All the complexes showed a superior inhibitory effect on the growth of A549 lung cancer cells among the three cancer cells screened. Complexes **3** and **6** comprising methoxy substituent have some marked effect on inhibition of cancer cell growth. Notably, complexes **4**−**6** outperformed the anticancer activity of cisplatin and 2-fold enhanced activity was found against LoVo and HuH cells in case of complex **6**.[20,38,39] When scrutinizing the results, it was found that the complexes containing a *p*-cymene moiety displayed a significant effect when compared to complexes **1**−**3** which contain a benzene moiety, implying the less hydrophobic interaction of Ru(II)−cymene complexes **4**−**6** with the cell membrane.[26] This observation highlighted the impact of arene moiety and electron-donating nature of the ligand in antiproliferation. Advantageously, the cancer cell growth inhibition capability of complexes **4**−**6** was significantly high when compared to other arene ruthenium complexes found in the literature as evidenced by the low IC_{50} values.[40,41] Despite this potency, the complexes were much less toxic toward the noncancerous 16HBE (human lung bronchial epithelium) cells, and the IC_{50} values were higher than those of cisplatin (Table 1). Expediently, the complexes exhibited better activity against the tested cells than other reported arene Ru(II) complexes containing different chelating ligands.[27] On the basis of the results, we have selected complexes **4**−**6** for further investigations.

Antiproliferative Activity by EdU Assay. Lung cancer (A549) is the leading cause of death worldwide. Therefore, we focused our interest to study the anticancer activity of complexes **4**−**6** against the A549 cell line. Furthermore, all the biochemical assay were performed for potent complexes **4**−**6** against A549 cancer cells. Since the complexes exhibit a higher cytotoxicity at IC_{50} concentration in a 72 h incubation period, we wish to perform all the biochemical assays with a minimal concentration (3.5 μM) for a 24 h incubation period in order to predict the apoptosis ratio of the particular cells. Furthermore, 5-ethynyl-2-deoxyuridine (EdU) incorporation assay was performed to evaluate the effect of potent Ru(II) *p*-cymene complexes **4**−**6** and cisplatin on prohibiting the cancer cell proliferation. One of the most proper ways to detect changes in cell proliferation is estimation of DNA synthesis. EdU is a thymidine analog comprising an alkyne terminal motif that subsumes only into the newly synthesized DNA of proliferating cancer cells when it is added to the growth media treated with the test compounds. After that, the synthesis of new DNA was quantified as green fluorescence by a copper-imparted click reaction between the fluorescent azide and the alkyne terminal of EdU. The percentage of EdU-stained cells was calculated on the basis of five randomly selected fields for each group after treatment with complexes **4**−**6** and cisplatin. After the treatment of the complexes, it has been observed that the percentage of cell proliferation was significantly decreased (Figure 5). It is inferred from the results that the complexes notably arrest A549 cell growth. Complex **6** exhibited higher antiproliferation which might be due to the presence of electron-donating nature of methoxy group.[42]

Apoptosis Induction by Dual Acridine Orange−Ethidium Bromide (AO-EB) Fluorescent Staining. Dual

https://dx.doi.org/10.1021/acs.organomet.0c00092
Organometallics XXXX, XXX, XXX−XXX

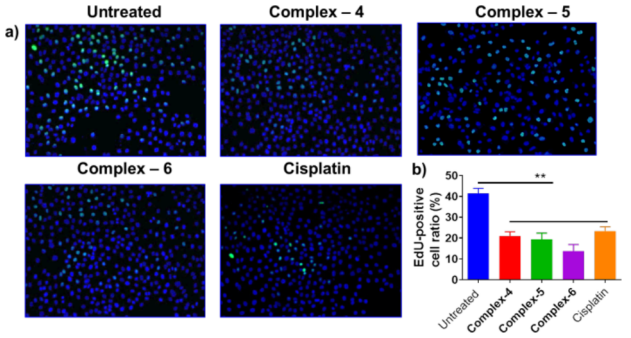

Figure 5. (a) Click-iTEdU assay for determining the proliferation of A549 cells. The cells were treated with complexes **4**–**6** and cisplatin (3.5 μM) for 24 h. (b) Quantification of cell proliferation.

AO-EB staining is a qualitative method to comprehend apoptosis and categorize live, early apoptotic, late apoptotic, and necrotic cells by documenting cell nuclear morphological changes by fluorescent images. AO can permeate the intact membrane of normal and early apoptotic cells and bind DNA, then fluorescing green, which is uniform in the case of the former case and as patches in the latter case due to differences in chromatin condensation. In contrast, EB is permeable only to the injured membranes of late apoptotic and dead cells and fluoresces as bright orange patches by binding with DNA fragments or apoptotic moieties and as uniform orange fluorescence in necrotic cells which have nuclear morphologies of viable cells. AO-EB-stained A549 cells were incubated with complexes **4**–**6**. As shown in Figure 6, the appearance of

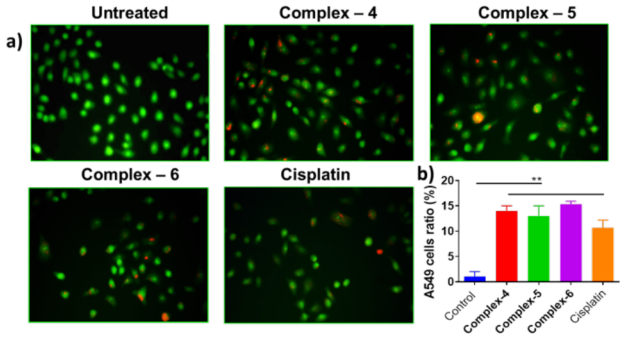

Figure 6. (a) AO-EB staining of A549 cells (3.5 μM, equiv concentrations) for 24 h. (b) Cell population in the microscopic field in AO-EB staining.

reddish orange fluorescence with fragmented chromatin after A549 cells were treated with complexes **4**–**6** and cisplatin suggests that complexes **4**–**6** largely induced apoptosis in A549 cells.[43]

Apoptosis Evaluation by Flow Cytometry. Apoptosis is the process of programmed cell death. The apoptosis-inducing property of arene Ru(II) complexes **4**–**6** was analyzed by flow cytometry using Alexa Fluor 488 Annexin V combined with propidium iodide (PI) staining assay in A549 cells. The cells at different stages, i.e., live cells, early apoptotic cells, and late apoptotic cells, were quantified in Annexin V^-/PI^-, Annexin V^+/PI^-, and Annexin V^+/PI^+ quadrants, respectively, using the fluorescence-activated cell sorting (FACS) methodology.[44] The ability of complexes **4**–**6** to induce apoptosis in the cancer cells was evaluated by flow cytometry. The A549 cells were treated with complexes **4**–**6** and cisplatin at 24 h. The flow cytometry result reveals that the cells are mainly in late apoptosis (Figure 7a,b), and complex **6** was more potent than

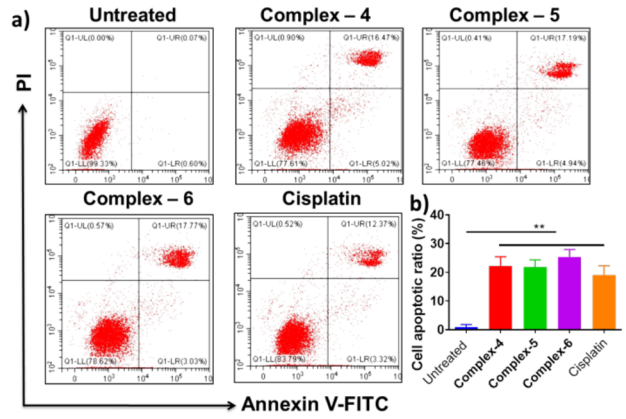

Figure 7. (a) Alexa Fluor 488 Annexin V/propidium iodide (PI) double-staining assay on A549 cells with complexes **4**–**6** and cisplatin. (b) Quantification of apoptotic cell ratio.

cisplatin with regard to inducing apoptosis. Furthermore, the flow cytometry analysis was performed at different concentrations of complex **6**. The cell death population in the quadrant represents cells undergoing apoptosis, which increased from 9% to 11 and 23% for 1, 2, and 3 μM complex respectively (Figure S45).[45] Recently, Subarkhan et al. recently reported the tetranuclear arene Ru(II) complexes induce late apoptosis on A549 cancer cells.[40a]

Cell Cycle Analysis by Flow Cytometry. Cell cycle progresses via different phases, namely, G0/G1 (Gap phase where cell grows and prepares for duplication), S (synthesis phase where DNA replicates), and G2/Mitosis (cell prepares to divide and results in two new daughter cells). The effectiveness of an anticancer drug depends on its ability to halt cancer cell division by cell cycle arrest in the aforesaid phases.[40a,46] Thence, complexes **4**–**6** were subjected to FACS to evaluate its influence on deregulating the cell cycle of A549. The percentage of A549 cells after treatment at 3.5 μM complexes **4**–**6** and cisplatin for 24 h in G0/G1 phase was decreased from 65.5% (untreated cells) to 14.5, 14.1, 13.6, and 15.2%, respectively (Figure 8). Complexes **4**–**6** elicited a strong S phase arrest in cells, accounting for 83.3, 86.7, and 87.3% of the cell population, respectively (untreated cells,

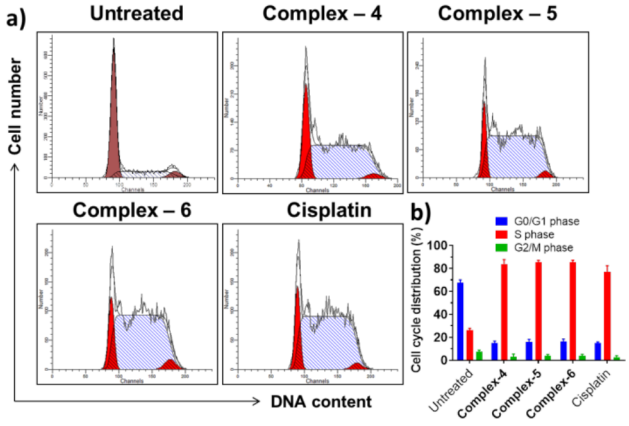

Figure 8. (a) FACS analysis on A549. (b) Distribution of the cell cycle.

https://dx.doi.org/10.1021/acs.organomet.0c00092
Organometallics XXXX, XXX, XXX−XXX

27.9%). Furthermore, dose-dependent cell cycle analysis was carried out for complex **6** and indicated the increase of apoptotic activity (Figure S46). Thus, the enhancement of the S phase arrest of cancer cells might result in apoptosis by disrupting the cell cycle.

Western Blot Analysis. Western blot technique was employed to authenticate the exact pathway behind the cancer cell death activity of the complex candidate. It is well-known that apoptotic proteins like BAX and antiapoptotic protein BCL-2 play a key role during the cell cycle.[47] BCL-2 is an intracellular membrane-associated oncogene responsible for extending cellular survival, which further confirmed that cell death occurred via apoptosis. BAX administers the release of cytochrome *c* from mitochondria to cytosol resulting in an increase of cytosolic cytochrome *c*. The expression levels of BAX and BCL-2 proteins were analyzed in the control and A549 cells treated with complex **6** (1, 2, and 3 μM). As portrayed in Figure 9, the diminishing expression level of the

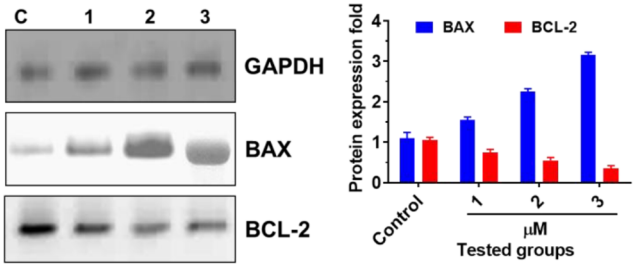

Figure 9. Western blot of BAX and BCL-2 proteins on A549 cells by complex **6**.

BCL-2 protein indicated the programmed cell death associated with complex **6**. Furthermore, the level of proapoptotic protein BAX in the cancer cells were exceptionally increased on the treatment with the complex. On the whole, the treatment of A549 cells with the complex induced the downregulation of BCL-2 and upregulation of Bax and thus confirmed that the complex **6** is a potential cancer cell apoptotic promoter. Upon increasing the concentration of complex **6** (1, 2, and 3 μM) the upregulation of BAX was increased, and the downregulation of BCL-2 decreased suggesting the dose-dependent cancer cell apoptotic activity of complex **6**. Furthermore, BAX displays 3-fold increase and BCL-2 shows a 0.3-fold decrease on treatment with 3 μM concentration.[34a,36b]

CONCLUSIONS

The present investigation highlights the synthesis of a new set of arene ruthenium(II) complexes bearing *N*,*N*-dimethylaminobenzhydrazone. Analytical, IR, UV−vis, NMR, and HR-MS methods have been used to establish the composition of the complexes. X-ray crystallographic study of complexes confirmed the bidentate chelation of benzhydrazone ligands and revealed the existence of pseudo-octahedral geometry around the ruthenium ion. MTT assay was utilized to evaluate *in vitro* cancer cell growth inhibition capacity of the complexes against A549 (lung carcinoma), LoVo (colon adenocarcinoma), HuH-7 (hepato cellular carcinoma) along with the noncancerous 16HBE (human lung bronchial epithelium) cells and compared with the effect of the standard drug cisplatin. *p*-Cymene complexes **4**−**6** outperformed benzene complexes **1**−**3** and cisplatin in all the cancer cells tested. In particular, 2-fold enhanced activity of complex **6** over that of cisplatin was found against LoVo and HuH-7 cells with low IC_{50} values 5.62 and 5.37 μM, respectively. The EdU incorporation assay confirmed that all the complexes inhibit cancer cell proliferation via minimal DNA synthesis. The cell membrane blebbing associated with apoptosis induced by the complexes was established by dual AO-EB fluorescent staining assay. Flow cytometry analyses confirmed that complexes **4**−**6** induce apoptosis in A549 cells, and the complexes have been shown to arrest A549 cell cycle in S phase. Furthermore, the results of Western blot analysis established that complex **6** is able to induce mitochondria-mediated apoptosis in A549 cells. Overall, the complexes presented herein exhibit considerably improved biological activity even at low concentrations. Therefore, this genre of complexes will be taken for further *in vivo* studies.

EXPERIMENTAL SECTION

Materials, methods, and crystal data collection were given in the Supporting Information (section S2).

Synthesis of Dimethylaminobenzoylhydrazone Ligands. The *p*-dimethylaminobenzaldehyde benzhydrazone ligands were synthesized by stirring an ethanolic mixture (25 mL) of 4-substituted benzhydrazides (0.1 mol) and *p*-dimethylaminobenzaldehyde (0.1 mol) at ambient temperature for 6 h. The completion of reaction resulted the formation of solid benzhydrazone ligands and which was collected by filtration, washed with ethanol then dried under vacuum. Analytically pure compounds were procured from recrystallization from methanol. NMR spectral data for the ligands were given in Supporting Information (Figures S13−S18).

Synthesis of Arene Ru(II) Benzhydrazone Complexes. The $[(\eta^6\text{-arene})RuCl_2]_2$ (arene: benzene or *p*-cymene) (0.5 mmol) precursor (1 mmol), *N*,*N*-dimethylaminobenzhydrazone ligand, and (1 mmol) triethylamine in 20 mL of benzene were combined and stirred for 5 h at ambient temperature. The progression of reaction was monitored through thin-layer chromatography, and column chromatographic separations of the reaction mixture afforded complexes **1**−**6** in 70:30% of hexane/ethyl acetate eluent.

*[Ru(L1)Cl(η^6-C_6H_6)] (**1**).* Brown solid. Yield = 75%; mp: 185 °C (with decomposition). Calcd: $C_{22}H_{22}N_3OClRu$: C, 54.22; H, 4.64; N, 8.72%. Found: C, 54.25; H, 4.61; N, 8.74%. IR (KBr, cm^{-1}): 1512 $\nu_{(C=N-N=C)}$, 1362 $\nu_{(C-O)}$. UV−vis (CH_3CN): λ_{max}, nm (ε_{max} dm^3 mol^{-1} cm^{-1}) 383 (1733), 292 (6342), 230 (14950). ^1H NMR (400 MHz, $CDCl_3$) (ppm): 8.88 (s, 1H, HC=N), 8.08 (m, H3, H5, H12, H16), 7.35 (m, H13, H14, H15), 6.77 (d, ^3J = 8 Hz, H2, H6), 3.08 (s, 6H, $N(CH_3)_2$). $^{13}C\{^1H\}$ NMR (100 MHz, $CDCl_3$, δ, ppm): 173.3 (C−O), 160.9 (C=N), 151.7 ($C-N(CH_3)_2$), 132.3 (Ar^{C14}), 132.1 (Ar^{C11}), 130.1 (Ar^{C13C15}), 128.6 (Ar^{C3C5}), 127.8 (Ar^{C12C16}), 121.7 (Ar^{C4}), 111.1 ($Ar^{C2,C6}$), 84.3 (CH of benzene), 40.1 ($N(CH_3)_2$), ESI-MS: *m/ z* 446.0804 $[M - Cl]^+$ (calcd *m/z* 481.0494).

*[Ru(L2)Cl(η^6-C_6H_6)] (**2**).* Brown solid. Yield = 78%, mp: 189 °C (with decomposition). Calcd: $C_{22}H_{21}N_3Cl_2ORu$: C, 51.22; H, 4.17; N, 8.17%. Found: C, 51.27; H, 4.11; N, 8.15%. IR (KBr, cm^{-1}): 1530 $\nu_{(C=N-N=C)}$, 1366 $\nu_{(C-O)}$. UV−vis (CH_3CN): λ_{max}, nm (ε_{max} dm^3 mol^{-1} cm^{-1}): 389 (2654), 291 (5510), 233 (10700). ^1H NMR (400 MHz, $CDCl_3$) (ppm): 8.80 (s, 1H, HC=N), 8.00 (t, ^3J = 16 Hz, H3, H5, H12, H16), 7.23 (d, ^3J = 8 Hz, H13, H15), 6.70 (d, ^3J = 8 Hz, H2, H6), 5.38 (s, 6H, CH-benzene), 3.01 (s, 6H, $N(CH_3)_2$). $^{13}C\{^1H\}$ NMR (100 MHz, $CDCl_3$, δ, ppm): 172.2 (C−O), 161.4 (C=N), 151.8 ($C-N(CH_3)_2$), 136.2 (Ar^{C14}), 132.2 ($Ar^{C12,C16}$), 130.0 ($Ar^{C13,C15}$), 128.1 ($Ar^{C3,C5}$), 128.0 (Ar^{C11}) 121.4 (Ar^{C4}), 111.1 ($Ar^{C2,C6}$) 84.3 (CH of benzene), 40.1 ($N(CH_3)_2$), ESI-MS: *m/z* 516.0173 $[M + H]^+$ (calcd *m/z* 515.0105).

*[Ru(L3)Cl(η^6-C_6H_6)] (**3**).* Brown solid. Yield = 81%, mp: 202 °C (with decomposition). Calcd: $C_{23}H_{24}N_3O_2ClRu$: C, 61.32; H, 4.08; N, 4.93%. Found: C, 61.34 H, 4.04; N, 4.95%. IR (KBr, cm^{-1}): 1500 $\nu_{(C=N-N=C)}$, 1363 $\nu_{(C-O)}$. UV−vis (CH_3CN): λ_{max}, nm (ε_{max} dm^3 mol^{-1} cm^{-1}): 387 (2114), 293 (5649), 233 (10611). ^1H NMR (400 MHz, $CDCl_3$) (ppm): 8.85 (s, 1H, HC=N), 8.05 (m, H3, H5, H12,

https://dx.doi.org/10.1021/acs.organomet.0c00092
Organometallics XXXX, XXX, XXX−XXX

H16), 6.85 (d, ^3J = 12 Hz, H13, H15), 6.76 (d, ^3J = 12 Hz, H2, H6), 5.42 (s, 6H, CH−benzene), 3.07 (s, 6H, $N(CH_3)_2$), 3.82 (s, 3H, OCH_3). $^{13}C\{^1H\}$ NMR (100 MHz, $CDCl_3$, δ, ppm): 173.2 (C−O), 162.0 (C═N), 160.1 (Ar^{C14}), 151.6 (C−$N(CH_3)_2$), 132.2 ($Ar^{C12,C16}$), 130.3 ($Ar^{C3,C5}$), 124.7 (Ar^{C4}), 122.0 (Ar^{C11}), 113.1 ($Ar^{C13,C15}$), 111.1 ($Ar^{C2,C6}$), 84.2 (CH of benzene), 55.3 (OCH_3) 40.1 ($N(CH_3)_2$). ESI-MS: m/z 476.0908 $[M - Cl]^+$ (calcd m/z 511.0600).

[Ru(L1)Cl(η^6-p-cymene)] (**4**). Red-brown solid. Yield = 85%, mp: 210 °C (with decomposition). Calcd: $C_{26}H_{30}N_3OClRu$: C, 64.47; H, 5.24; N, 4.70%. Found: C, 64.49; H, 5.26; N, 4.68%. IR (KBr, cm^{-1}): 1516 $\nu_{(C=N-N=C)}$, 1361 $\nu_{(C-O)}$. UV−vis (CH_3CN): λ_{max}, nm (ε_{max} dm^3 mol^{-1} cm^{-1}) 387 (2513), 294 (6140), 231 (11460). ^1H NMR (400 MHz, $CDCl_3$) (ppm): 8.88 (s, 1H, HC═N), 8.06 (m, H3, H5, H12, H16), 7.34 (m, H13, H14, H15), 6.76 (d, ^3J = 12 Hz, H2, H6), 5.43 (d, J = 6 Hz, 1H, p-cymene-H), 5.34 (d, J = 6 Hz, 1H, p-cymene−H), 4.96 (d, J = 6.4 Hz, 1H, p-cymene−H), 4.72 (d, J = 6 Hz, 1H, p-cymene−H), (3.07, s, 6H, −$N(CH_3)_2$), 2.67 (m, 1H, p-cym $CH(CH_3)_2$), 2.30 (s, 3H, p-cymene-CCH_3), 1.13 (dd, J = 12.4 Hz, 6H, p-cymene−$CH(CH_3)_2$). $^{13}C\{1H\}$NMR (100 MHz, $CDCl_3$, δ, ppm): 173.1 (C−O), 160.3 (C═N), 151.5 (C−$N(CH_3)_2$), 132.4 (Ar^{C14}), 132.3 (Ar^{C11}), 130.0 (Ar^{C13C15}), 128.6 (Ar^{C3C5}), 127.8 (Ar^{C12C16}), 121.7 (Ar^{C4}), 111.1 ($Ar^{C2,C6}$), 101.4 and 101.1 (quaternary carbons of p-cymene), 80.9, 81.3, 82.1, 84.6 (Ar carbons of p-cymene), 40.1 ($N(CH_3)_2$), 30.9 (CH, p-cymene), 22.6, 22.0 ($2CH_3$, p-cymene), 18.9 (CH_3, p-cymene), ESI-MS: m/z 538.1190 $(M + H)^+$(calcd m/z 537.1120).

[Ru(L2)Cl(η^6-p-cymene)] (**5**). Red-brown solid. Yield = 89%, mp: 205 °C (with decomposition). Calcd: $C_{26}H_{29}N_3Cl_2ORu$: C, 61.15; H, 4.49; N, 4.46%. Found: C, 61.13; H, 4.53; N, 4.46%. IR (KBr, cm^{-1}): 1519 $\nu_{(C=N-N=C)}$, 1340 $\nu_{(C-O)}$. UV−vis (CH_3CN): λ_{max}, nm (ε_{max} dm^3 mol^{-1} cm^{-1}) 388 (1457), 287 (5564), 236 (10096). ^1H NMR (400 MHz, $CDCl_3$) (ppm): 8.85 (s, 1H, HC═N), 8.02 (m, H3, H5, H12, H16), 7.28 (d, ^3J = 8 Hz, H13, H15), 6.75 (d, ^3J = 8 Hz, H2, H6), 5.42 (d, J = 5.6 Hz, 1H, p-cymene−H), 5.33 (d, J = 5.6 Hz, 1H, p-cymene−H), 4.96 (d, J = 5.6 Hz, 1H, p-cymene−H), 4.72 (d, J = 5.6 Hz, 1H, p-cymene−H), (3.07, s, 6H, −$N(CH_3)_2$), 2.64 (m, 1H, p-cymene−$CH(CH_3)_2$), 2.30 (s, 3H, p-cymene−CCH_3), 1.11−1.13 (dd, J = 12 Hz, 6H, p-cymene−$CH(CH_3)_2$). $^{13}C\{^1H\}$ NMR (100 MHz, $CDCl_3$, δ, ppm): 171.9 (C−O), 160.6 (C═N), 151.6 (C−$N(CH_3)_2$), 136.0 (Ar^{C14}), 132.3 ($Ar^{C12,C16}$), 131.0 ($Ar^{C13,C15}$), 130.0 ($Ar^{C3,C5}$), 128.0 (Ar^{C11}) 122.0 (Ar^{C4}), 111.1 ($Ar^{C2,C6}$), 101.5 and 101.1 (quaternary carbons of p-cymene), 84.5, 82.1, 81.3, 80.9 (Ar carbons of p-cymene), 40.1 ($N(CH_3)_2$), 30.9 (CH, p-cymene), 22.6, 21.9 ($2CH_3$, p-cymene), 18.9 (CH_3, p-cymene). ESI-MS: m/z 572.0800 $(M + H)^+$(calcd m/z 571.0712).

[Ru(L3)Cl(η^6-p-cymene)] (**6**). Red-brown solid. Yield = 90%, mp: 196 °C (with decomposition). Calcd: $C_{27}H_{32}N_3O_2ClRu$: C, 63.50; H, 5.01; N, 4.49%. Found: C, 63.48; H, 5.01; N, 4.48%. IR (KBr, cm^{-1}): 1508 $\nu_{(C=N-N=C)}$, 1370 $\nu_{(C-O)}$. UV−vis (CH_3CN): λ_{max}, nm (ε_{max} dm^3 mol^{-1} cm^{-1}) 385 (1222), 290 (5975), 234 (16589). ^1H NMR (400 MHz, $CDCl_3$) (ppm): 8.86 (s, 1H, HC═N), 8.03 (d, ^3J = 8 Hz, H3, H5, H12, H16), 6.84 (d, ^3J = 8 Hz, H13, H15), 6.76 (d, ^3J = 8 Hz, H2, H6), 5.42 (d, J = 6 Hz, 1H, p-cymene−H), 5.33 (d, J = 5.6 Hz, 1H, p-cymene−H), 4.95 (d, J = 6 Hz, 1H, p-cymene−H), 4.69 (d, J = 6 Hz, 1H, p-cymene−H), (3.07, s, 6H, −$N(CH_3)_2$), 3.81 (s, 3H, OCH_3), 2.67 (m, 1H, p-cymene−$CH(CH_3)_2$), 2.29 (s, 3H, p-cymene−CCH_3), 1.15 (dd, J = 13.2 Hz, 6H, p-cymene−$CH(CH_3)_2$). $^{13}C\{^1H\}$ NMR (100 MHz, $CDCl_3$, δ, ppm): 173.0 (C−O), 161.2 (C═N), 159.6 (Ar^{C14}), 151.4 (C−$N(CH_3)_2$), 132.2 ($Ar^{C12,C16}$), 130.3 ($Ar^{C3,C5}$), 125.0 (Ar^{C4}), 122.3 (Ar^{C11}), 113.1 ($Ar^{C13,C15}$), 111.1 ($Ar^{C2,C6}$), 101.4 and 101.0 (quaternary carbons of p-cymene), 84.6, 82.1, 81.4, 80.9 (Ar carbons of p-cymene), 55.3 (OCH_3), 40.2 ($N(CH_3)_2$), 30.9 (CH, p-cymene), 22.6, 22.0 ($2CH_3$, p-cymene), 18.9 (CH_3, p-cymene). ESI-MS: m/z 568.1295 $(M + H)^+$ (calcd m/z 567.1226).

■ ASSOCIATED CONTENT

Supporting Information

The Supporting Information is available free of charge at https://pubs.acs.org/doi/10.1021/acs.organomet.0c00092.

Complete details and procedures for chemistry and biology experiments. Characterization data for ligands, tables for crystallographic data, refinement parameters, selected bond lengths and bond angles. Figures illustrating the FT-IR, NMR, UV−vis, HR-MS, stability studies and MTT results of the new compounds (PDF)

Accession Codes

CCDC 1565996 and 1833167 contain the supplementary crystallographic data for this paper. These data can be obtained free of charge via www.ccdc.cam.ac.uk/data_request/cif, or by emailing data_request@ccdc.cam.ac.uk, or by contacting The Cambridge Crystallographic Data Centre, 12 Union Road, Cambridge CB2 1EZ, UK; fax: +44 1223 336033.

■ AUTHOR INFORMATION

Corresponding Author

Rengan Ramesh − *Centre for Organometallic Chemistry, School of Chemistry, Bharathidasan University, Tiruchirappalli 620 024, India;* orcid.org/0000-0002-0257-8792; Email: ramesh_bdu@yahoo.com

Authors

Sundarraman Balaji − *Centre for Organometallic Chemistry, School of Chemistry, Bharathidasan University, Tiruchirappalli 620 024, India*

Mohamed Kasim Mohamed Subarkhan − *The First Affiliated Hospital, Key Laboratory of Combined Multi-Organ Transplantation, Ministry of Public Health, School of Medicine, Zhejiang University, Hangzhou 310003, PR China*

Hangxiang Wang − *The First Affiliated Hospital, Key Laboratory of Combined Multi-Organ Transplantation, Ministry of Public Health, School of Medicine, Zhejiang University, Hangzhou 310003, PR China;* orcid.org/0000-0001-6370-9728

David Semeril − *Laboratoire de Chimie Inorganique et Catalyse, Institut de Chimie, UMR 7177, CNRS, Universite de Strasbourg, Strasbourg 67008, France*

Complete contact information is available at: https://pubs.acs.org/10.1021/acs.organomet.0c00092

Notes

The authors declare no competing financial interest.

■ ACKNOWLEDGMENTS

The authors thank DST−FIST, New Delhi, for HR-MS and NMR facilities at the School of Chemistry, Bharathidasan University, Tiruchirappalli. M.S.K. gratefully acknowledges the Zhejiang Province Fund (No. 519000-X81801) for the financial support.

■ REFERENCES

(1) Kelland, L. The resurgence of platinum-based cancer chemotherapy. *Nat. Rev. Cancer* **2007**, *7*, 573−584.

(2) Judson, I.; Cerny, T.; Epelbaum, R.; Dunlop, D.; Smyth, J.; Schaefer, B.; Roelvink, M.; Kaplan, S.; Hanauske, A. Phase II trial of the oral platinum complex JM216 in non-small-cell lung cancer: An EORTC early clinical studies group investigation. *Annals of Oncology* **1997**, *8*, 604−606.

(3) Koepf-Maier, P.; Koepf, H. Non-platinum group metal antitumor agents. History, current status, and perspectives. *Chem. Rev.* **1987**, *87*, 1137−1152.
(4) (a) Mari, C.; Pierroz, V.; Ferrari, S.; Gasser, G. Combination of Ru(II) complexes and light: new frontiers in cancer therapy. *Chem. Sci.* **2015**, *6*, 2660−2686. (b) Mari, C.; Gasser, G. Lightening up Ruthenium Complexes to Fight Cancer? *Chimia* **2015**, *69*, 176−181. (c) Kostova, I. Ruthenium Complexes as Anticancer Agents. *Curr. Med. Chem.* **2006**, *13*, 1085−1107.
(5) Reisner, E.; Arion, V. B.; Keppler, B. K.; Pombeiro, A. J. L. Electron-transfer activated metal-based anticancer drugs. *Inorg. Chim. Acta* **2008**, *361*, 1569−1583.
(6) Biersack, B. Anticancer Activity and Modes of Action of (arene) ruthenium(II) Complexes Coordinated to C-, N-, and O-ligands. *Mini-Rev. Med. Chem.* **2016**, *16*, 804−814.
(7) Bergamo, A.; Gaiddon, C.; Schellens, J. H. M.; Beijnen, J. H.; Sava, G. Approaching tumour therapy beyond platinum drugs: Status of the art and perspectives of ruthenium drug candidates. *J. Inorg. Biochem.* **2012**, *106*, 90−99.
(8) Bergamo, A.; Sava, G. Ruthenium anticancer compounds: myths and realities of the emerging metal-based drugs. *Dalton Trans.* **2011**, *40*, 7817−7823.
(9) (a) Hartinger, C. G.; Zorbas-Seifried, S.; Jakupec, M. A.; Kynast, B.; Zorbas, H.; Keppler, B. K. From bench to bedside - preclinical and early clinical development of the anticancer agent indazolium trans-[tetrachlorobis(1H-indazole)ruthenate(III)] (KP1019 or FFC14A). *J. Inorg. Biochem.* **2006**, *100*, 891−904. (b) Hartinger, C. G.; Jakupec, M. A.; Zorbas-Seifried, S.; Groessl, M.; Egger, A.; Berger, W.; Zorbas, H.; Dyson, P. J.; Keppler, B. K. KP1019, A New Redox-Active Anticancer Agent - Preclinical Development and Results of a Clinical Phase I Study in Tumor Patients. *Chem. Biodiversity* **2008**, *5*, 2140−2155.
(10) (a) Bergamo, A.; Messori, L.; Piccioli, F.; Cocchietto, M.; Sava, G. Biological role of adduct formation of the ruthenium(III) complex NAMI-A with serum albumin and serum transferrin, Invest. *Invest. New Drugs* **2003**, *21*, 401−411. (b) Alessio, E.; Mestroni, G.; Bergamo, A.; Sava, G. Ruthenium Antimetastatic Agents. *Curr. Top. Med. Chem.* **2004**, *4*, 1525−1535. (c) Alessio, E. Thirty Years of the Drug Candidate NAMI-A and the Myths in the Field of Ruthenium Anticancer Compounds: A Personal Perspective. *Eur. J. Inorg. Chem.* **2017**, *2017*, 1549−1560.
(11) Zeng, L.; Gupta, P.; Chen, Y.; Wang, E.; Ji, L.; Chao, H.; Chen, Z. S. The development of anticancer ruthenium(II) complexes: from single molecule compounds to nanomaterials. *Chem. Soc. Rev.* **2017**, *46*, 5771−5804.
(12) Smithen, D. A.; Yin, H.; Beh, M. H. R.; Hetu, M.; Cameron, T. S.; McFarland, S. A.; Thompson, A. Synthesis and Photobiological Activity of Ru(II) Dyads Derived from Pyrrole-2-carboxylate Thionoesters. *Inorg. Chem.* **2017**, *56*, 4121−4132.
(13) Hayward, R. L.; Schornagel, Q. C.; Tente, R.; Macpherson, J. S.; Aird, R. E.; Guichard, S.; Habtemariam, A.; Sadler, P.; Jodrell, D. I. Investigation of the role of Bax, p21/Waf1 and p53 as determinants of cellular responses in HCT116 colorectal cancer cells exposed to the novel cytotoxic ruthenium(II) organometallic agent, RM175. *Cancer Chemother. Pharmacol.* **2005**, *55*, 577−583.
(14) Chatterjee, S.; Kundu, S.; Bhattacharyya, A.; Hartinger, C. G.; Dyson, P. J. The ruthenium(II)-arene compound RAPTA-C induces apoptosis in EAC cells through mitochondrial and p53-JNK pathways. *JBIC, J. Biol. Inorg. Chem.* **2008**, *13*, 1149−1155.
(15) Thota, S.; Rodrigues, D. A.; Crans, D. C.; Barreiro, E. J. Ru(II) Compounds: Next-Generation Anticancer Metallotherapeutics. *J. Med. Chem.* **2018**, *61*, 5805−5821.
(16) (a) Zeng, L.; Gupta, P.; Chen, Y.; Wang, E.; Ji, L.; Chao, H.; Chen, Z.-S. The development of anticancer ruthenium(II) complexes: from single molecule compounds to nanomaterials. *Chem. Soc. Rev.* **2017**, *46*, 5771−5804. (b) Zhang, P.; Sadler, P. J. Advances in the design of organometallic anticancer complexes. *J. Organomet. Chem.* **2017**, *839*, 5−14. (c) Murray, B. S.; Babak, M. V.; Hartinger, C. G.; Dyson, P. J. The Development of RAPTA Compounds for the Treatment of Tumors. *Coord. Chem. Rev.* **2016**, *306*, 86−114. (d) Morris, R. E.; Aird, R. E.; del Socorro Murdoch, P.; Chen, H.; Cummings, J.; Hughes, N. D.; Parsons, S.; Parkin, A.; Boyd, G.; Jodrell, D. I.; Sadler, P. J. Inhibition of Cancer Cell Growth by Ruthenium(II) Arene Complexes. *J. Med. Chem.* **2001**, *44*, 3616−3621. (e) Adhireksan, Z.; Davey, G. E.; Campomanes, P.; Groessl, M.; Clavel, C. M.; Yu, H.; Nazarov, A. A.; Yeo, C. H.; Ang, W. H.; Droge, P.; Rothlisberger, U.; Dyson, P. J.; Davey, C. A. Ligand substitutions between ruthenium-cymene compounds can control protein versus DNA targeting and anticancer activity. *Nat. Commun.* **2014**, *5*, 3462. (f) Berndsen, R. H.; Weiss, A.; Abdul, U. K.; Wong, T. J.; Meraldi, P.; Griffioen, A. W.; Dyson, P. J.; Nowak-Sliwinska, P. Combination of ruthenium(II)-arene complex [Ru(η^6-p-cymene)Cl_2(pta)] (RAPTAC) and the epidermal growth factor receptor inhibitor erlotinib results in efficient angiostatic and antitumor activity. *Sci. Rep.* **2017**, *7*, 43005.
(17) (a) Martínez-Peña, F.; Infante-Tadeo, S.; Habtemariam, A.; Pizarro, A. M. Reversible pH-Responsive Behavior of Ruthenium(II) Arene Complexes with Tethered Carboxylate. *Inorg. Chem.* **2018**, *57*, 5657−5668. (b) Zhao, J.; Zhang, D.; Hua, W.; Li, W.; Xu, G.; Gou, S. Anticancer Activity of Bifunctional Organometallic Ru(II) Arene Complexes Containing a 7-Hydroxycoumarin Group. *Organometallics* **2018**, *37*, 441−447. (c) Chen, F.; Romero-Canelón, I.; Soldevila-Barreda, J. J.; Song, J.-I.; Coverdale, J. P. C.; Clarkson, G. J.; Kasparkova, J.; Habtemariam, A.; Wills, M.; Brabec, V.; Sadler, P. J. Transfer Hydrogenation and Antiproliferative Activity of Tethered Half-Sandwich Organoruthenium Catalysts. *Organometallics* **2018**, *37*, 1555−1566. (d) Li, J. J.; Tian, Z.; Ge, X.; Xu, Z.; Feng, Y.; Liu, Z. Design, synthesis, and evaluation of fluorine and Naphthyridinee Based half-sandwich organoiridium/ruthenium complexes with bioimaging and anticancer activity. *Eur. J. Med. Chem.* **2019**, *163*, 830−839. (e) Ma, W.; Guo, L.; Tian, Z.; Zhang, S.; He, X.; Li, J.; Yang, Y.; Liu, Z. Rhodamine-modified Fluorescent Half-sandwich Iridium and Ruthenium Complexes: Potential Application as Bioimaging and Anticancer Agents. *Dalton Trans.* **2019**, *48*, 4788−4793.
(18) Grgurić-Šipka, S.; Ivanović, I.; Rakić, G.; Todorović, N.; Gligorijević, N.; Radulović, S.; Arion, V. B.; Keppler, B. K.; Tešić, Ž. L. Ruthenium(II)-arene complexes with functionalized pyridines: Synthesis, characterization and cytotoxic activity. *Eur. J. Med. Chem.* **2010**, *45*, 1051−1058.
(19) Martínez-Peña, F.; Infante-Tadeo, S.; Habtemariam, A.; Pizarro, A. M. Reversible pH-Responsive Behavior of Ruthenium(II) Arene Complexes with Tethered Carboxylate. *Inorg. Chem.* **2018**, *57*, 5657−5668.
(20) Pettinari, R.; Marchetti, F.; Di Nicola, C.; Pettinari, C.; Galindo, A.; Petrelli, R.; Cappellacci, L.; Cuccioloni, M.; Bonfili, L.; Eleuteri, A. M.; Guedes da Silva, M. F. C.; Pombeiro, A. J. L. Ligand Design for N, O- or N, N-Pyrazolone-Based Hydrazones Ruthenium-(II)-Arene Complexes and Investigation of Their Anticancer Activity. *Inorg. Chem.* **2018**, *57*, 14123−14133.
(21) Rahman, F.-U.; Bhatti, M. Z.; Ali, A.; Duong, H.-Q.; Zhang, Y.; Ji, X.; Lin, Y.; Wang, H.; Li, Z.-T.; Zhang, D.-W. DimetallicRu(II) arene complexes appended on bis-salicylaldimine induce cancer cell death and suppress invasion via p53-dependent signaling. *Eur. J. Med. Chem.* **2018**, *157*, 1480−1490.
(22) Yamada, S. Advancement in stereochemical aspects of Schiff base metal complexes. *Coord. Chem. Rev.* **1999**, *190−192*, 537−555.
(23) Yan, Y. K.; Melchart, M.; Habtemariam, A.; Sadler, P. J. Organometallic chemistry, biology and medicine: ruthenium arene anticancer complexes. *Chem. Commun.* **2005**, 4764−4776.
(24) Kandile, N. G.; Mohamed, M. I.; Zaky, H.; Mohamed, H. M. Novel pyridazine derivatives: Synthesis and antimicrobial activity evaluation. *Eur. J. Med. Chem.* **2009**, *44*, 1989−1996.
(25) Hruskova, K.; Kovarikova, P.; Bendova, P.; Haskova, P.; Mackova, E.; Stariat, J.; Vavrova, A.; Vavrova, K.; Simunek, T. Synthesis and Initial in Vitro Evaluations of Novel Antioxidant Aroylhydrazone Iron Chelators with Increased Stability against Plasma Hydrolysis. *Chem. Res. Toxicol.* **2011**, *24*, 290−302.

https://dx.doi.org/10.1021/acs.organomet.0c00092
Organometallics XXXX, XXX, XXX−XXX

(26) (a) Leyva, L.; Sirlin, C.; Rubio, L.; Franco, C.; Lagadec, R. L.; Spencer, J.; Bischoff, P.; Gaiddon, C.; Loeffler, J.-P.; Pfeffer, M. Synthesis of Cycloruthenated Compounds as Potential Anticancer Agents. *Eur. J. Inorg. Chem.* **2007**, *2007*, 3055−3066. (b) Fetzer, L.; Boff, B.; Ali, M.; Xiangjun, M.; Collin, J.-P.; Sirlin, C.; Gaiddon, C.; Pfeffer, M. Library of second-generation cycloruthenated compounds and evaluation of their biological properties as potential anticancer drugs: Passing the nanomolar barrier. *Dalton Trans.* **2011**, *40*, 8869−8878. (c) Mohamed Kasim, M. S.; Sundar, S.; Rengan, R. Synthesis and structure of new binuclear ruthenium(II) arene benzilbis-(benzoylhydrazone) complexes: investigation on antiproliferative activity and apoptosis induction. *Inorg. Chem. Front.* **2018**, *5*, 585−596.

(27) (a) Ribeiro, I. G.; da Silva, K. C. M.; Parrini, S. C.; de Miranda, A. L. P.; Fraga, C. A. M.; Barreiro, E. J. Synthesis and antinociceptive properties of new structurally planned imidazo[1,2-a]pyridine 3-acylarylhydrazone derivatives. *Eur. J. Med. Chem.* **1998**, *33*, 225−235.

(28) Lima, P. C.; Lima, L. M.; da Silva, K. C. M.; Léda, P. H. O.; de Miranda, A. L. P.; Fraga, C. A. M.; Barreiro, E. J. Synthesis and analgesic activity of novel N-acylarylhydrazones and isosters, derived from natural safrole. *Eur. J. Med. Chem.* **2000**, *35*, 187−203.

(29) Pettinari, R.; Pettinari, C.; Marchetti, F.; Skelton, B. W.; White, A. H.; Bonfili, L.; Cuccioloni, M.; Mozzicafreddo, M.; Cecarini, V.; Angeletti, M.; Nabissi, M.; Eleuteri, A. M. Arene-Ruthenium(II) Acylpyrazolonato Complexes: Apoptosis-Promoting Effects on Human Cancer Cells. *J. Med. Chem.* **2014**, *57*, 4532−4542.

(30) Kurzwernhart, A.; Kandioller, W.; Bächler, S.; Bartel, C.; Martic, S.; Buczkowska, M.; Mühlgassner, G.; Jakupec, M. A.; Kraatz, H.-B.; Bednarski, P. J.; Arion, V. B.; Marko, D.; Keppler, B. K.; Hartinger, C. G. Structure-Activity Relationships of Targeted RuII(η6-p-Cymene) Anticancer Complexes with Flavonol-Derived Ligands. *J. Med. Chem.* **2012**, *55*, 10512−10522.

(31) Su, W.; Qian, Q.; Li, P.; Lei, X.; Xiao, Q.; Huang, S.; Huang, C.; Cui, J. Synthesis, Characterization, and Anticancer Activity of a Series of Ketone-N4-Substituted Thiosemicarbazones and Their Ruthenium(II) Arene Complexes. *Inorg. Chem.* **2013**, *52*, 12440−12449.

(32) Haghdoost, M. M.; Guard, J.; Golbaghi, G.; Castonguay, A. Anticancer Activity and Catalytic Potential of Ruthenium(II)-Arene Complexes with N, O-Donor Ligands. *Inorg. Chem.* **2018**, *57*, 7558−7567.

(33) Gatti, A.; Habtemariam, A.; Romero-Canelón, I.; Song, J.; Heer, B.; Clarkson, G. J.; Rogolino, D.; Sadler, P. J.; Carcelli, M. Half-Sandwich Arene Ruthenium(II) and Osmium(II) Thiosemicarbazone Complexes: Solution Behavior and Antiproliferative Activity. *Organometallics* **2018**, *37*, 891−899.

(34) (a) Subarkhan, M. K. M.; Ramesh, R. Ruthenium(II) arene complexes containing benzhydrazone ligands: synthesis, structure and antiproliferative activity. *Inorg. Chem. Front.* **2016**, *3*, 1245−1255. (b) Raj Kumar, R.; Ramesh, R.; Małecki, J. G. Synthesis and structure of arene ruthenium(II) benzhydrazone complexes: Antiproliferative activity, apoptosis induction and cell cycle analysis. *J. Organomet. Chem.* **2018**, *862*, 95−104.

(35) Haghdoost, M.; Golbaghi, G.; Letourneau, M.; Patten, S. A.; Castonguay, A. Lipophilicity-antiproliferative activity relationship study leads to the preparation of a ruthenium(II) arene complex with considerable *in vitro* cytotoxicity against cancer cells and a lower *in vivo* toxicity in zebrafish embryos than clinically approved cisplatin. *Eur. J. Med. Chem.* **2017**, *132*, 282−293.

(36) (a) Mohan, N.; Mohamed Subarkhan, M. K.; Ramesh, R. Synthesis, antiproliferative activity and apoptosis-promoting effects of arene ruthenium(II) complexes with N, O chelating ligands. *J. Organomet. Chem.* **2018**, *859*, 124−131. (b) Mohamed Subarkhan, M. K.; Ramesh, R.; Liu, Y. Synthesis and molecular structure of arene ruthenium(II) benzhydrazone complexes: impact of substitution at the chelating ligand and arene moiety on antiproliferative activity. *New J. Chem.* **2016**, *40*, 9813−9823. (c) Pandiarajan, D.; Ramesh, R. Ruthenium(II) half-sandwich complexes containing thioamides: Synthesis, structures and catalytic transfer hydrogenation of ketones. *J. Organomet. Chem.* **2013**, *723*, 26−35.

(37) (a) Gupta, R. K.; Sharma, G.; Pandey, R.; Kumar, A.; Koch, B.; Li, P.-Z.; Xu, Q.; Pandey, D. S. DNA/protein binding, molecular docking, and in vitro anticancer activity of some thioether-dipyrrinato complexes. *Inorg. Chem.* **2013**, *52*, 13984−13996. (b) Gupta, R. K.; Pandey, R.; Sharma, G.; Prasad, R.; Koch, B.; Srikrishna, S.; Li, P.-Z.; Xu, Q.; Pandey, D. S. DNA Binding and Anti-Cancer Activity of Redox-Active Heteroleptic Piano-Stool Ru(II), Rh(III), and Ir(III) Complexes Containing 4(2-Methoxypyridyl)phenyldipyrromethene. *Inorg. Chem.* **2013**, *52*, 3687−3698. (c) OECD. *Guidelines for Testing of Chemicals*; OECD: Paris, France, 1995; Vol. *107*.

(38) (a) Vajpayee, V.; Yang, Y. J.; Kang, S. C.; Kim, H.; Kim, I. S.; Wang, M.; Stang, P. J.; Chi, K.-W. Hexanuclear self-assembled arene-ruthenium nano-prismatic cages: potential anticancer agents. *Chem. Commun.* **2011**, *47*, 5184−5186. (b) Kubanik, M.; Holtkamp, H.; Söhnel, T.; Jamieson, S. M. F.; Hartinger, C. G. Impact of the Halogen Substitution Pattern on the Biological Activity of Organo-ruthenium 8-Hydroxyquinoline Anticancer Agents. *Organometallics* **2015**, *34*, 5658−5668. (c) Gupta, R. K.; Sharma, G.; Pandey, R.; Kumar, A.; Koch, B.; Li, P.-Z.; Xu, Q.; Pandey, D. S. DNA/Protein Binding, Molecular Docking, and in Vitro Anticancer Activity of Some Thioether-Dipyrrinato Complexes. *Inorg. Chem.* **2013**, *52*, 13984−13996. (d) Mukhopadhyay, S.; Gupta, R. K.; Paitandi, R. P.; Rana, N. K.; Sharma, G.; Koch, B.; Rana, L. K.; Hundal, M. S.; Pandey, D. S. Synthesis, Structure, DNA/Protein Binding, and Anticancer Activity of Some Half-Sandwich Cyclometalated Rh(III) and Ir(III) Complexes. *Organometallics* **2015**, *34*, 4491−4506.

(39) Morris, R. E.; Aird, R. E.; del Socorro Murdoch, P.; Chen, H.; Cummings, J.; Hughes, N. D.; Parsons, S.; Parkin, A.; Boyd, G.; Jodrell, D. I.; Sadler, P. J. Inhibition of Cancer Cell Growth by Ruthenium(II) Arene Complexes. *J. Med. Chem.* **2001**, *44*, 3616−3621.

(40) (a) Mohamed Subarkhan, M. K.; Ren, L.; Xie, B.; Chen, C.; Wang, Y.; Wang, H. Novel tetranuclear ruthenium(II) arene complexes showing potent cytotoxic and antimetastatic activity as well as low toxicity in vivo. *Eur. J. Med. Chem.* **2019**, *179*, 246−256. (b) Čanovic, P.; Simovic, A.; Radisavljevic, S.; Bratsos, I.; Demitri, N.; Mitrovic, M.; Zelen, I.; Bugarčic, Ž. D. Impact of aromaticity on anticancer activity of polypyridylruthenium(II) complexes: Synthesis, structure, DNA/proteinbinding, lipophilicity and anticancer activity. *JBIC, J. Biol. Inorg. Chem.* **2017**, *22* (7), 1007−1028. (c) Habtemariam, A.; Melchart, M.; Fernández, R.; Parsons, S.; Oswald, I. D. H.; Parkin, A.; Fabbiani, F. P. A.; Davidson, J. E.; Dawson, A.; Aird, R. E.; Jodrell, D. I.; Sadler, P. J. Structure-Activity Relationships for Cytotoxic Ruthenium(II) Arene Complexes Containing N, N-, N, O-, and O, O-Chelating Ligands. *J. Med. Chem.* **2006**, *49*, 6858−6868.

(41) Ruiz, J.; Rodríguez, V.; Cutillas, N.; Espinosa, A.; Hannon, M. J. A Potent Ruthenium(II) Antitumor Complex Bearing a Lipophilic Levonorgestrel Group. *Inorg. Chem.* **2011**, *50*, 9164−9171.

(42) (a) Liu, Z.; Romero-Canelón, I.; Habtemariam, A.; Clarkson, G. J.; Sadler, P. J. Potent Half-Sandwich Iridium(III) Anticancer Complexes Containing C^N-Chelated and Pyridine Ligands. *Organometallics* **2014**, *33*, 5324−5333. (b) Mohan, N.; Muthumari, S.; Ramesh, R. Synthesis, structure and anticancer activity of (η6-benzene) ruthenium(II) complexes containing aroylhydrazone ligands. *J. Organomet. Chem.* **2016**, *807*, 45−51.

(43) He, L.; Liao, S.-Y.; Tan, C.-P.; Ye, R.-R.; Xu, Y.-W.; Zhao, M.; Ji, L.-N.; Mao, Z.-W. Ruthenium-Arene-β-Carboline Complexes as Potent Inhibitors of Cyclin-Dependent Kinase 1: Synthesis, Characterization and Anticancer Mechanism Studies. *Chem. - Eur. J.* **2013**, *19*, 12152−12160.

(44) Mohamed Subarkhan, M.; Prabhu, R. N.; Raj Kumar, R.; Ramesh, R. Antiproliferative activity of cationic and neutral thiosemicarbazone copper(II) complexes. *RSC Adv.* **2016**, *6*, 25082−25093.

(45) Wang, H.; Chen, J.; Xu, C.; Shi, L.; Tayier, M.; Zhou, J.; Zhang, J.; Wu, J.; Ye, Z.; Fang, T.; Han, W. Cancer Nanomedicines Stabilized by π-π Stacking between HeterodimericProdrugs Enable Exception-

https://dx.doi.org/10.1021/acs.organomet.0c00092
Organometallics XXXX, XXX, XXX−XXX

ally High Drug Loading Capacity and Safer Delivery of Drug Combinations. *Theranostics* **2017**, *7*, 3638−3652.
(46) Wang, J.; Wang, H.; Li, J.; Liu, Z.; Xie, H.; Wei, X.; Lu, D.; Zhuang, R.; Xu, X.; Zheng, S. iRGD-Decorated Polymeric Nanoparticles for the Efficient Delivery of Vandetanib to Hepatocellular Carcinoma: Preparation and in Vitro and in Vivo Evaluation. *ACS Appl. Mater. Interfaces* **2016**, *8*, 19228−19237.
(47) Yuan, Y.; Xu, L.; Dai, S.; Wang, M.; Wang, H. A facile supramolecular approach to fabricate multifunctional upconversion nanoparticles as a versatile platform for drug loading, in vivo delivery and tumor imaging, A facile supramolecular approach to fabricate multifunctional upconversion nanoparticles as a versatile platform for drug loading, in vivo delivery and tumor imaging. *J. Mater. Chem. B* **2017**, *5*, 2425−2435.

https://dx.doi.org/10.1021/acs.organomet.0c00092
Organometallics XXXX, XXX, XXX−XXX